Biophysical Chemistry 10(1979) 305–318

THE BINDING OF A NEUTRAL AROMATIC MOLECULE TO A NEGATIVELY-CHARGED LIPID MEMBRANE. II. KINETICS AND MECHANISM ☆

Paul WOOLLEY *
Magdalene College, Cambridge, England

and

Hartmut DIEBLER
Max-Planck-Institut für biophysikalische Chemie, Göttingen-Nikolausberg, West Germany

Received 4 December 1978
Revised manuscript received 6 March 1979

The kinetics of the binding of the fluorescence indicator N-phenyl naphthylamine to bilayer vesicles of C_{12}-methylphosphatidic acid have been investigated by means of the temperature-jump relaxation technique utilizing fluorescence light detection. Single-exponential relaxation curves were observed, with time constants in the range 0.2–3 ms. The concentration dependence of the relaxation time yielded an apparent association rate constant (expressed in terms of monomeric phospholipid) of $k_{on} = 5 \times 10^6\ M^{-1}\ s^{-1}$ in aqueous solution at 25°. The activation energy and viscosity dependence associated with the binding rate show that this process is actually diffusion-controlled. The theory of diffusion-controlled reactions then allows a determination of the average size of the bilayer vesicles and of the true rate constant for the association of the indicator molecules with the vesicles. Assuming spherical geometry for the vesicles, the values are: $r_{ves} = 190$ Å, which corresponds to 20000 lipid molecules per vesicle and $k'_{on} = 1 \times 10^{11}\ M^{-1}\ s^{-1}$ (25°). The correctness of this size-determination was confirmed semi-quantitatively by electron microscopy. Since in fact a distribution of vesicle sizes must be present, a discussion is included of the relaxation function which the system is expected to take in the general case. Biological implications of diffusion control for the transport of non-polar substances and for lipid mixing are indicated.

1. Introduction

For reasons given in the preceding paper [1], the interaction of the neutral fluorescence indicator N-phenyl naphthylamine (NPN, fig. 1) with bilayer structures of lipids is of considerable interest. This paper deals with the kinetics of this interaction, i.e. with the rates with which NPN binds to and dissociates from the lipid membrane. Knowledge of these processes is not only a prerequisite for the use of NPN as an indica-

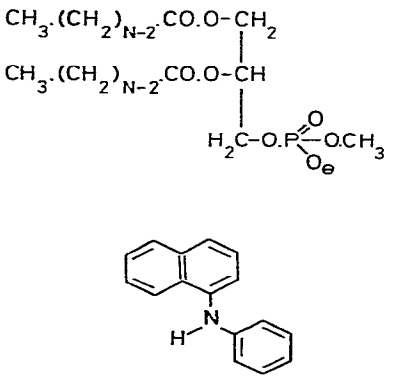

Fig. 1. Structures of C_N-MPA and NPN. In NPN there is restricted rotation about the C–N bonds; owing to steric interference the phenyl and naphthyl rings are not quite coplanar.

☆ Presented at the Chemical Society conference "Fast Reactions in Solution" (Cranfield, England) in September, 1977.

* Present address: Max-Planck-Institut für molekulare Genetik, Berlin 33.

tor in kinetic studies of the phase transition of lipid bilayers; it will also contribute towards a general picture of the kinetics of interaction between lipid membranes and other organic molecules, a subject with obvious biological significance. As in the equilibrium studies [1], the lipid methyl phosphatidic acid (MPA, fig. 1) was used in this investigation.

2. Materials

MPA was prepared and checked for purity as described in the preceding paper [1], which also describes the preparation of MPA vesicles by sonicating suspensions of the lipid. Stock dispersions of MPA were stored at 5° without added salt. Under these conditions a two-week old dispersion displayed a deviation in its rate constants of only ~10% compared with their values when the dispersion was fresh. Since, even with these precautions, not all dispersions gave identical kinetic results, sets of kinetic experiments were carried out in the shortest feasible time (< 3 days) using the same stock dispersion.

NPN (Eastman), sodium chloride (Merck, "Suprapur" grade), $Na_2HPO_4 \cdot 2H_2O$ (Merck, p.a.) and sucrose (Serva, p.a.) were used without further purification. Water was used direct from a quartz double still.

3. Method

The kinetic studies were carried out by means of the temperature-jump relaxation technique with fluorescence light intensity detection. The instrument was a version of that described before [2], improved by C.R. Rabl. The cell had a heating volume of 0.7 ml and an optical pathlength (along both axes) of 7 mm. A capacitor of 0.05 microfarads charged to 15 kV thus gave a temperature jump of 1.9 degrees. The vesicles in the dispersion appeared to suffer no ill-effects due to the temperature jump or the associated high current and field as long as they had been prepared in the standard manner (see sect. 2.3 of ref. [1]). The alternative, gentler sonication procedure produced vesicles which appeared to be disrupted if the applied voltage exceeded 10 kV (temperature jump = 0.85°).

All kinetic experiments were carried out on dispersions containing 0.1 M sodium chloride (for conductivity) and 0.001 M disodium hydrogen phosphate, the latter acting as buffer for the pH which was 7.6 ± 0.3 in all cases. The concentration of MPA was varied between 5×10^{-5} and 5×10^{-4} M, that of NPN was usually 2×10^{-5} M. In one series of experiments the MPA dispersion further contained sucrose in order to reveal the effect of solvent viscosity on the kinetics.

MPA dispersion and salt solutions were mixed to make 990 μl and immediately before measurement 10 μl NPN in methanol were added. After thorough mixing the solution was transferred to the temperature-jump cell and degassed (experience showed this to be necessary). After thermal equilibration in the cell housing (40 minutes) measurements were completed within a further 20 minutes. Approximately 5 shots were made on each solution. If more than 10 shots were made, or if the fluorescence excitation beam was allowed to pass for a total of more than 30 seconds, then loss of the NPN by photolysis became noticeable (ca. 1 second of illumination was required for each shot, with a few seconds at the beginning for manual balancing of the amplifier).

The resistance of the cell was 350 ohms at 10°C and 190 ohms at 45°C. The heating time-constants expected (RC/2) are thus 9 and 5 μs respectively. This accords with the heating time observed (see sect. 4.1). The relaxation time of the reaction was always at least two orders of magnitude higher, so no interference was seen, even in the presence of sucrose, which increased the resistance to 1800 ohms.

The light source was a xenon-mercury lamp with a Schoeffel GM 250 monochromator. The line at 366 nm was used for excitation and a 400 nm cut-off filter was employed to filter out the small quantity of light scattered by the vesicles and the cell walls. The lamp was defocussed in order to reduce the rate of photolysis of the NPN, which otherwise manifested itself as a constant slope superimposed over the exponential relaxation curve, making evaluation of the relaxation times much less accurate. In order to check that photolysis was not reappearing, baseline sweeps were made with each shot. Results were recorded using a Tektronix 549 storage oscilloscope and photographed onto 35 mm film.

The relaxation times and amplitudes were evaluated with an exponential simulator built by C.R. Rabl. A facility for correcting slightly-sloping baselines was

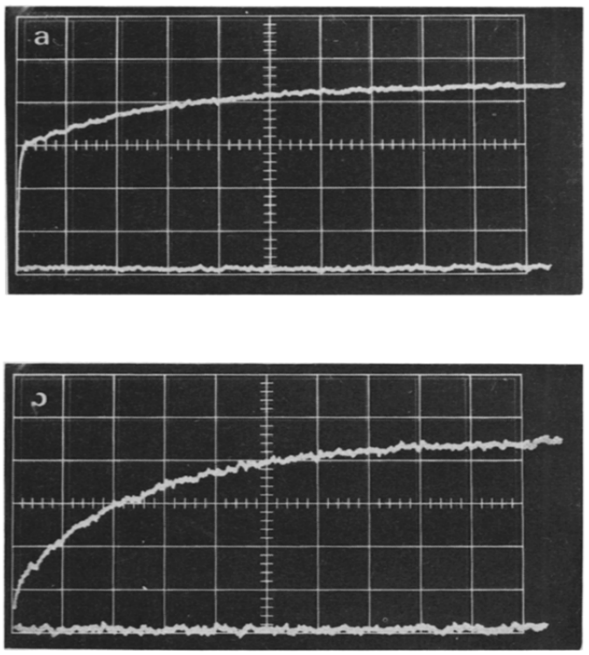

Fig. 2. Typical relaxation curves seen following the temperature jump. (a) Fast heating effect and slow chemical relaxation. Horizontal scale 500 μs/div., vertical 200 mV/div. (b) Delayed triggering reveals chemical effect alone. Horizontal scale 500 μs/div., vertical 100 mV/div., time offset 20 μs.

also built into the simulator. Relaxation times measured on one solution were mutually consistent to 5% accuracy in most cases.

Temperatures given were measured within the temperature-jump cell and are accurate to ±0.2 degrees.

4. Results

4.1. Kinetics of NPN binding to C_{12}-MPA

The binding of NPN below the transition temperature of the lipid bilayers is weak and of uncertain nature [1]. Kinetic studies were therefore carried out with C_{12}-MPA vesicles in the fluid state, since bilayers of this lipid have a transition temperature of 5°C; this is sufficiently low to allow a wide temperature range to be covered. At issue were the rate law, the number of steps, the effect of temperature, the effect of solvent viscosity, and the relaxation amplitude.

Some representative relaxation curves are shown in fig. 2.

The number of relaxation times was investigated by varying the deflection speed of the oscillograph from ca. 5 μs per division (full scale = 10 divisions) to ca. 50 ms per division. At high deflection speeds a rapid change in the fluorescence signal was observed which correlated well with the heating time of the solution (a few μs, see sect. 3). Since the absolute quantum yield of the dye is temperature-dependent (e.g. fig. 2 of ref. [1]), this rapid change was attributed to the change in quantum yield Q during the heating time. In support of this assignment, the sign of the rapid effect corresponded to a decreasing fluorescence intensity with increasing temperature, as it should do (*loc. cit.*). Furthermore, since the output of the amplifier through which the fluorescence signal was fed was kept by adjustment of the gain at 20 V, this output was independent of the amount of NPN bound and of its quantum yield. Consequently the amplitude of the fast change in fluorescence should be given in volts by $(20\ \Delta Q/Q)$, which is independent of concentration. (The contribution of free NPN to the fluorescence signal is negligible.) In a typical series of experiments, over which the MPA concentration was varied by a factor of ten, the fast signal remained constant at 582 mV ± 3%, and variations in it showed no correlation with the MPA concentration. From table 1 of ref. [1] $(\mathrm{d}\Delta F_{max}/\mathrm{d}T)/\Delta F_{max}$ at 30°C is $-0.0168\ \mathrm{deg}^{-1}$, predicting a fast signal change, due to heating, of 638 mV. This consistency confirms our assignment of the fast change to a heating effect alone.

Following the heating effect in the relaxation spectrum came a smaller change in fluorescence output which we attributed to the binding of NPN to the MPA. In almost all of the curves fitted with the exponential simulator, the correspondence of the slower effect with a single exponential function was good. In a very few cases it was possible to find a slightly better fit to the observed relaxation using two exponential functions than using one; however the relaxation times were close together and a resolution of these, or even a confident assertion of the presence of systematic deviation from the single exponential function, was not possible. In the evaluation of results the best-fitting single exponential was taken in all cases. The accuracy of fitting was greatly increased by electronic suppression of the rapid heating effect; the fluorescence signal was cut

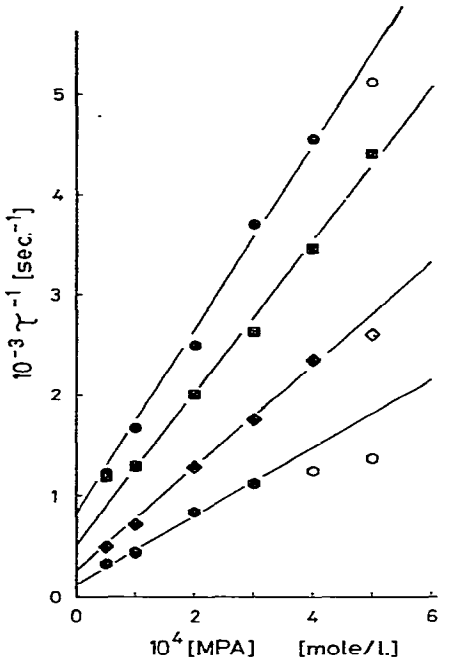

Fig. 3. Reciprocal relaxation time of NPN/MPA binding as a function of MPA concentration and temperature. ([NaCl], 0.1 M; [NPN], 2×10^{-5} M; pH 8) (circles, 48.6°C; squares, 36.5°C; diamonds, 26.5°C; hexagons, 14.2°C; open symbols were omitted from the statistical analysis, as the amplitudes were very small in these cases. The lines are from one-parameter least-squares refinement (sect. 5.1.1).

off for several (usually 20) μs after the temperature jump and the signal at the moment of cut-on used as the zero point for the oscilloscope trace. Thus the smaller, slower effect could be amplified to fill the oscilloscope screen (fig. 2b).

No further, slower relaxation effects were found.

The rate/concentration law of the slow effect is in fact extremely simple, as fig. 3 shows; the reciprocal relaxation time is linearly related to the concentration of MPA. Equating *pro tem.* the gradient and intercept with an apparent association and dissociation rate constant respectively, we observe as expected that both of these increase with increasing temperature.

In fig. 4 a similar family of curves is shown, measured at one temperature in the presence of varying concentrations of sucrose. The sucrose raises the viscosity of the solution and reduces the rate of the reaction.

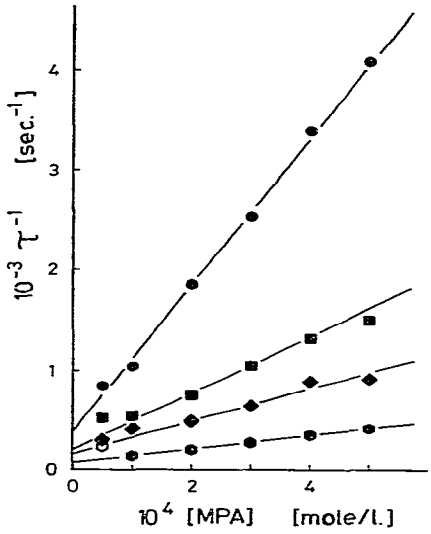

Fig. 4. Reciprocal relaxation time of NPN/MPA binding as a function of MPA and sucrose concentrations. ([NaCl], 0.1 M; [NPN], 2×10^{-5} M; pH 8; 31.9°C). (Circles, no sucrose; squares, 30% sucrose; diamonds, 40%; hexagons, 50%; open symbol was omitted from the statistical analysis.)

In most experiments the relaxation amplitude was not measured accurately since this required additional shots. However in one series both the amplitude and the time of the relaxation were measured, and fig. 5 shows that they are directly proportional to one another.

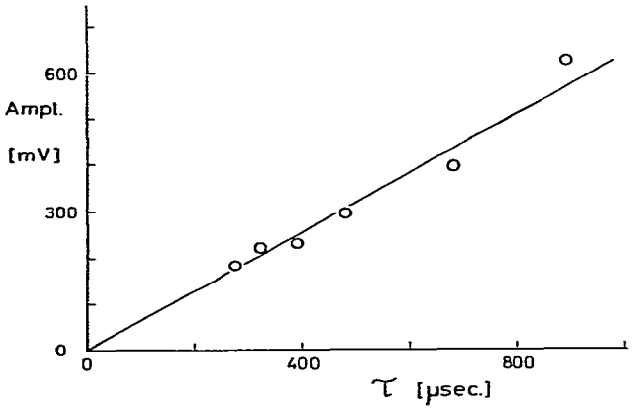

Fig. 5. Relaxation amplitude plotted against relaxation time. ([NaCl], 0.1 M; [NPN], 2×10^{-5} M; [MPA], varied from 4×10^{-5} to 4.4×10^{-4} M; 32°C, pH 8).

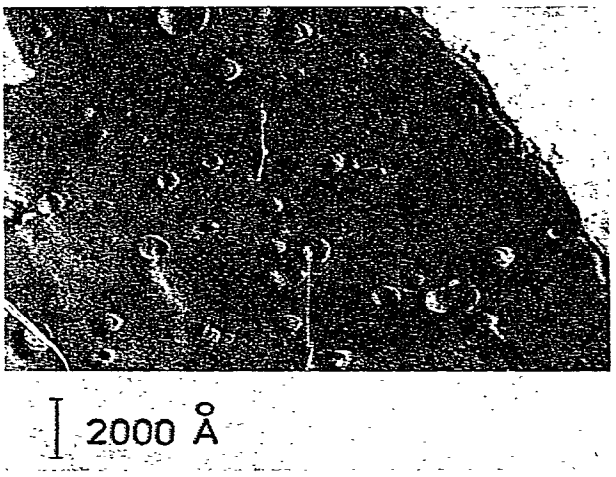

Fig. 6. Typical electron micrograph of C_{12}-MPA vesicles prepared in the standard manner.

4.2. Electron microscopy

This was carried out by K. Harlos. Fig. 6 shows a typical electron micrograph of a dispersion of C_{12}-MPA prepared in the standard manner. Two preparations with sodium chloride at the working concentration for the kinetic experiments (0.1 M) were examined and two without sodium chloride. In no case were large multilayered structures observed such as have been seen with unsonicated MPA [3]. The particle radius may be estimated from the pictures, but the error will be high, since the shadowing tends to exaggerate the size of some particles, while partial embedding in the ice will make others appear too small.

5. Discussion

5.1. Kinetics of binding of NPN to MPA

In this section we shall adduce evidence that the entry of NPN into a fluid MPA bilayer and its exit therefrom can be described as occurring in a single step and that the binding rate is determined by diffusion through the external, aqueous medium.

5.1.1. The rate law

It has already been shown (sect. 4.1) that the association—dissociation reaction is characterised by a single observable relaxation time, the reciprocal of which is linearly related to the total concentration of MPA in the concentration range studied (fig. 3) and which is sensitive to the viscosity of the solution (fig. 4). To interpret the kinetic law we require a model for the binding reaction.

To express the amount of lipid membrane in solution one can use either the concentration of vesicles, [Ves], or the concentration of lipid molecules, [MPA], If the number of lipid molecules in each vesicle is n, then [MPA] $= n$ [Ves]. In this section we shall assume that all the vesicles are of the same size, i.e., n is constant. When a distribution of sizes is present in a dispersion the situation becomes more complex (see appendix II). Since [MPA] is known accurately and n (and therefore [Ves]) is not, we shall adopt the convention that rate and equilibrium constants based on [Ves] are denoted with a prime and those based on [MPA] are not.

Since the binding sites are present in the aggregated form of vesicles, the latter species are the particles actually encountered by the indicator molecules, and we may write eq. (1), in which the forward and reverse reactions, with rate constants denoted by k'_{on} and k'_{off}, describe respectively the association of an NPN molecule with a vesicle and the dissociation therefrom. Each vesicle has a very large number

$$NPN_{free} + Ves \underset{k'_{off}}{\overset{k'_{on}}{\rightleftharpoons}} NPN_{bound} \qquad (1)$$

of binding sites, so it is not "used up" by a binding step as shown in eq. (1), i.e. the vesicle concentration is constant during the relaxation process. Therefore the reciprocal relaxation time is given simply by eq. (2a) [4,5],

$$\tau^{-1} = k'_{on}\,[Ves] + k'_{off} \qquad (2a)$$

$$\tau^{-1} = k_{on}\,[MPA] + k_{off} \qquad (2b)$$

which may be rewritten in the experimentally accessible form eq. (2b) ($k'_{on} = nk_{on}$; $k'_{off} = k_{off}$), the parameters of which are the gradient and intercept of a plot such as fig. 3.

A schematic model of the mechanism of the binding process may be formulated in the following way:

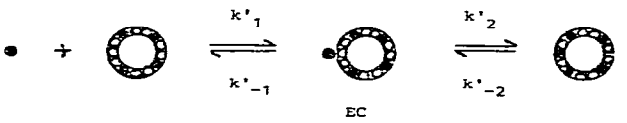

An NPN molecule approaches a vesicle, whose binding sites are partially occupied, and forms an encounter complex EC which then reacts to give NPN_{bound}. Applying the steady-state approximation to the concentration of EC yields eq. (3) for the rate of reaction.

$$\frac{d[NPN_{bound}]}{dt} = \frac{k'_1 k'_2}{k'_{-1} + k'_2}[NPN_{free}][Ves] - \frac{k'_{-1}k'_{-2}}{k'_{-1} + k'_2}[NPN_{bound}] \quad (3)$$

With [Ves] constant, the expression for τ^{-1} calculated from this rate equation takes the form of eq. (2a), with $k'_{on} = k'_1 k'_2/(k'_{-1} + k'_2)$ and $k'_{off} = k'_{-1}k'_{-2}/(k'_{-1} + k'_2)$. The value of k'_2 is expected to depend on the degree of occupation of the vesicle, at least at higher degrees of occupation, and the same might apply to the reverse rate constant k'_{-2} if the rate with which an NPN molecule leaves the vesicle depends on whether the neighbouring sites are occupied or not.

As long as $k'_2 \gg k'_{-1}$, the diffusion-controlled encounter of the reactants is rate-determining, so that eq. (4a) applies ($K'_1 = k'_1/k'_{-1}$; $K'_2 = k'_2/k'_{-2}$). We may also write eq. (4b), in analogy with eq. (2b).

$$\tau^{-1} = k'_1[Ves] + k'_{-1}/K'_2 \quad (4a)$$

$$\tau^{-1} = (k'_1/n)[MPA] + k'_{-1}/K'_2 \quad (4b)$$

However, if $k'_{-1} \gg k'_2$, the entry of NPN is rate-determining and the binding is activation-controlled. This condition leads to eqs. (5a) and (5b).

$$\tau^{-1} = k'_2 K'_1[Ves] + k'_{-2} \quad (5a)$$

$$\tau^{-1} = (k'_2 K'_1/n)[MPA] + k'_{-2} \quad (5b)$$

Both expressions, (4b) and (5b), are consistent with the experimental observations which have been plotted in fig. 3 and are kinetically indistinguishable, so another criterion must be used to show whether the association is diffusion-controlled. It may be noted at this stage that possible variations of k'_2 and k'_{-2} at high occupation densities might affect the rates of association and dissociation in the case of activation-controlled binding (eq. (5a)) and that of dissociation in the case of diffusion-controlled reaction (eq. (4a)). Thus the linear relation between τ^{-1} and [MPA] could break down at high degrees of occupation. However, although the equilibrium data show that under the conditions of the kinetic studies a large fraction of all binding sites is occupied by NPN (about 13–60%, depending on concentrations and assuming $m \approx 4$ (ref. [1], sect. 4.3), there is no significant deviation from linearity in the plots (fig. 3) corresponding to eqs. (4b) and (5b).

It is easily shown that the binding and rate constants are linked by eq. (6)

$$K = \frac{K'}{n} = \frac{k_{on}}{k_{off}} = \frac{k'_{on}}{k'_{off}n} = \frac{k'_1 k'_2}{k'_{-1}k'_{-2}n} \quad (6)$$

where the experimentally accessible quantities are K, k_{on} and k_{off}. In using eq. (2b) (or (4b) or (5b)) to evaluate the experimental results in fig. 3, therefore, either one may assume the values of K yielded by the titration experiments [1] and carry out a one-parameter fit, or else one may use the gradient and intercept in a two-parameter fit to find both k_{on} and k_{off} and then compare the ratio of these with the titrimetrically-determined K values. Table 1 shows the results of a one-parameter evaluation in which the expression $k_{off} = k_{on}/K$ was substituted into eq. (2b) and then k_{on} adjusted to give the best fit to the points of fig. 3 by the criterion of least squares; k_{off} was then calculated from k_{on}/K. In table 2 the results of a two-parameter evaluation are shown and the k_{on}/k_{off} ratios are com-

Table 1
One-parameter evaluation of k_{on} and k_{off}

Temperature (°C)	10^{-3} K [a] (M^{-1})	10^{-6} k_{on} [b] (M^{-1} s^{-1})	k_{off} [c] (s^{-1})
48.6	11.2	9.19 ± 5%	821
36.5	15.1	7.58 ± 5%	502
26.5	19.7	5.09 ± 3%	259
14.2	27.9	3.37 ± 6%	121

a) Calculated from $\Delta H = -4.88$ kcal/mole and $\Delta S = 3.36$ cal/deg-mole, determined in ref. [1], sect. 4.1.
b) Obtained from the data points in fig. 3. Errors are standard deviations.
c) Calculated using $k_{off} = k_{on}/K$; the standard deviations are the same as for k_{on}.

Table 2
Two-parameter evaluation of k_{on} and k_{off}

Temperature (°C)	$10^{-6}\ k_{on}$ [a,c] ($M^{-1}\ s^{-1}$)	k_{off} [a,d] (s^{-1})	$10^{-3}\ K$ [b] (M^{-1})
48.6	9.76 ± 3%	670	14.6
36.5	7.28 ± 5%	600	12.1
26.5	5.30 ± 2%	200	26.1
14.2	3.25 ± 7%	150	22.0

a) Obtained from the data points in fig. 3. Errors are standard deviations.
b) Compare with the smoothed values obtained from titration shown in table 1, second column.
c) Calculated Arrhenius activation energy, 5.9 ± 0.3 kcal/mole; cf. corresponding value from one-parameter evaluation, 5.5 ± 0.4 kcal/mole.
d) Calculated Arrhenius activation energy 9.0 ± 2.3 kcal/mole; implies a ΔH for binding of 3.1 ± ca. 2.3 kcal/mole; cf. ΔH from titration, 4.88 kcal/mole.

pared with the K values from titration. This comparison shows that within the accuracy of the determination the kinematically- and titrimetrically-determined values of K are mutually compatible, and provide no grounds for postulating a different rate law. The experimental error is clearly associated with k_{off}.

Fig. 7 shows an Arrhenius plot for k_{on} using the data from table 1. The activation energy (E_A) inferred from this plot is 5.5 ± 0.4 kcal/mole. The rate constants for 25°C are: k_{on}, $5.0 \times 10^6\ M^{-1}\ s^{-1}$; k_{off}, $250\ s^{-1}$. By combining the titration data with the activation energy of k_{on}, the activation energy for k_{off} is found to be 10.4 kcal/mole.

5.1.2. Effect of solvent viscosity

Since solvent viscosity does not enter into the rate expression for an activation-controlled reaction [6], the observed dependence of the reaction rate (fig. 4) upon viscosity implies at least partial diffusion control. If the reaction is completely diffusion-controlled [7,8] then the rate of the "on" step will be inversely proportional to the viscosity η of the solvent. That such a relationship exists here is shown by fig. 8, based on values taken from fig. 4 using eq. (2b) (one-parameter fitting, $k_{off} = k_{on}/K$; K values from table 1 of ref. [1]). A finite intercept indicates partial diffusion-control (eq. 7 [8,9]) and is the rate with

$$k^{-1} = k_0^{-1} + \eta/qRT \qquad (7)$$

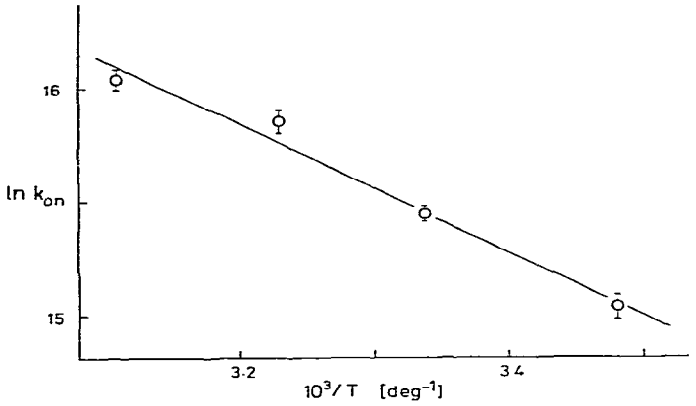

Fig. 7. Arrhenius plot of k_{on}. Data from fig. 3 (table 1).

which the reaction would proceed in an infinitely mobile solvent, i.e., the activation-controlled value. Here this is immeasurably high ($k_0^{-1} \to 0$). The association reaction is therefore diffusion-controlled in water. A plot (not shown) of log k_{on} versus log η had a gradient of −0.95 ± 0.04 (theoretical value −1.0). The factor q (eq. (7)) is about 4 if both of the reactant molecules and the solvent molecules are of the same size; in our case, involving vesicles, q is expected to be appreciably larger. A plot of $1/k'_{on}$ versus η, where $k'_{on} = nk_{on}$ with $n \approx 20\,000$ (see below), yields $q = 54$. This is of the expected magnitude considering the large difference in size between the reaction partners [10].

If k'_{on} is given by qRT/η the apparent energy of activation is calculated to be 4.5 kcal/mole by using tabulated values of η [11]. The experimentally-determined activation energy of the binding reaction is 5.5

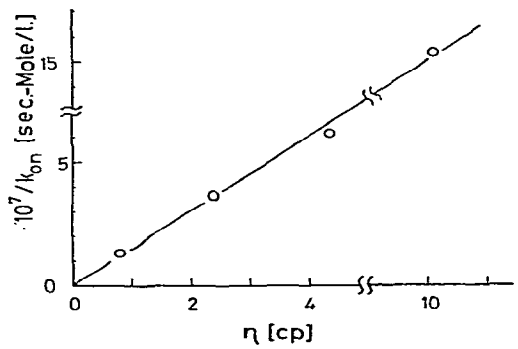

Fig. 8. Relationship between k_{on} and solvent viscosity. Data from fig. 4. For interpretation, see sect. 5.1.2.

kcal/mole, in fair agreement with the value calculated. This provides additional support for the diffusion-control hypothesis.

If the reaction is diffusion-controlled then information may be obtained about the size of the particles in the dispersion. The relevant equations are derived and discussed in appendices I and II.

From eqs. (A4) and (A5) respectively we may calculate the number of lipid molecules in one spherical or disc-shaped vesicle. The average radius of an NPN molecule is 4 Å, so that from the Stokes–Einstein equation, assuming a viscosity of 0.8 cp and a temperature of 300 K, the diffusion coefficient of NPN is 7×10^{-6} cm^2 s^{-1}. Then, from eq. (A4) the average radius of the vesicles if they are spherical is 190 Å and the number n of phospholipid molecules they contain is 20 000. If the vesicles are disc-shaped then the corresponding figures, from equation A5, are 490 Å and 33 000 molecules. The electron micrographs showed particles with an apparent mean diameter of ca 400–700 Å, but such estimates are very uncertain, as discussed above (sect. 4.2 and fig. 6). However, the correspondence is on the surface satisfactory.

If this estimate of particle size is correct, then k'_{on} has a value at 25°C of 1.0×10^{11} M^{-1} s^{-1} if the vesicles are spherical and 1.6×10^{11} M^{-1} s^{-1} if they are disc-shaped.

As one would expect, we are dealing in these experiments not with a dispersion of vesicles of identical size, but with a distribution of vesicle sizes. The effect of this on the kinetics would be unimportant if they were not diffusion-controlled, but under diffusion control the dependence upon particle size of the rate constants can influence the form of the relaxation curve. The relationships concerned are derived in appendix II, with the conclusion that the relaxation curve at high lipid concentration is exponential as usual, giving an average relaxation time for the distribution, whereas the relaxation curve at low lipid concentration, where k_{off} predominates in the expression for τ^{-1}, is not exponential unless a single vesicle size is present.

It is normally not possible to resolve accurately two separate relaxation times superimposed upon one another unless they differ by a factor of ten or more, and it is difficult even to detect the fact that they are separate unless this factor exceeds three. Consequently for a narrow spread of particle sizes deviation from true exponentiality will be overlooked. In the kinetic experiments described here the lipid was usually in reasonable excess over NPN. In a very few cases there was slight deviation from exponential decay which could not be attributed to noise, etc. Such observations could not by systematically obtained. It is conceivable that these observations were due to the onset of deviation from the exponential law caused by a particularly broad distribution of vesicle radii in some dispersions.

5.1.3. Amplitude of the relaxation

For a simple equilibrium $A + B \rightleftharpoons C$, where C is a fluorescent species, the amplitude of the relaxation is expressed as $\Delta[C]/[C]$. For convenience, the static signal before the perturbation was brought to a fixed level by varying the gain, and the relaxation was measured relative to this. Since the equilibrium constant K is given by $[C]/[A][B]$, it may easily be shown by differentiation that the amplitude is related by eq. (8) to the change in equilibrium constant at the perturbation.

$$\frac{\Delta[C]}{[C]} = \frac{1}{[C]}\left(\frac{1}{[A]} + \frac{1}{[B]} + \frac{1}{[C]}\right)^{-1} \Delta \ln K \qquad (8)$$

Since the reciprocal relaxation time is given [4,5,12] by $k_{on}([A] + [B] + K^{-1})$, and since k_{on} equals $(k_{off}K)$, rearrangement gives eq. (9) for the relaxation amplitude of a simple association reaction.

$$\Delta[C]/[C] = \tau k_{off} \Delta \ln K \qquad (9)$$

(For a more general treatment, see ref. [13].) The fluorescence signal ΔF is measured in mV with respect to a quiescent signal of 20 V. Therefore, applying the usual thermodynamic relationships, we obtain expression (10) for ΔF in mV.

$$\Delta F = 20\,000\, k_{off} \frac{\Delta H}{RT^2} \cdot \Delta T \cdot \tau \qquad (10)$$

This linear relationship has already been shown in fig. 5 whence $\Delta F/\tau = 638$ V/s. Inserting the values for T (304 K), ΔT (1.9°C) and k_{off} (378 s^{-1}) leads to the value for ΔH of −8.2 kcal/mole. This is 67% higher than the value obtained from titration (−4.9 kcal/mole). The agreement is not satisfactory, but we are unable at present to account for the discrepancy. One explanation of the discrepancy could in theory be the existence of a second, much slower step. However this is implausible in view of the satisfactory agreement between the equilibrium constants determined by static

titration and by two-parameter analysis of the kinetic data.

5.2. The mechanism of the binding reaction

Evidence that binding may be regarded as taking place in a single step is (i) the existence of a single relaxation time associated with the binding process, (ii) the direct proportionality between the time and the amplitude of this relaxation, (iii) the linear relationship between the reciprocal relaxation time and the concentration of MPA, (iv) the agreement within experimental error between statically- and kinetically-determined binding equilibrium constants and, less convincing, (v) the approximate agreement between values for the enthalpy of binding determined from the temperature dependence of the binding constant and from the relaxation amplitude.

Evidence that the binding is diffusion-controlled lies in (i) the relationship between rate and viscosity, (ii) the consistence of the activation energy with that expected from diffusion control and (iii) the agreement between the particle size calculated from the rate and the approximate particle size as seen under the electron microscope. In the following discussion some of the consequences of diffusion control will be examined.

It is unusual for a reaction to be diffusion-controlled unless the amount of molecular movement and electronic rearrangement required between collision and attainment of the transition state is small. Typical diffusion-controlled reactions are protonation [14] and the binding of strong Lewis-basic ligands to metal ions with vacant co-ordination sites [8].

We must therefore postulate that the transition state for the incorporation of an NPN guest molecule into the MPA membrane is not very different from the "collision complex" in which the two species are barely in contact with each other. This is illustrated in fig. 9, in which the transition complex is pictured as the situation in which an incoming NPN molecule (fig. 9a) has lost some of its surrounding water by penetrating a very short distance into the membrane (fig. 9b). This is a reasonable representation of the transition complex, since in its formation the two main hindrances to the binding of the guest molecule have been overcome: the immobilisation of NPN, which is entropically disadvantageous (energetically favourable loss of the

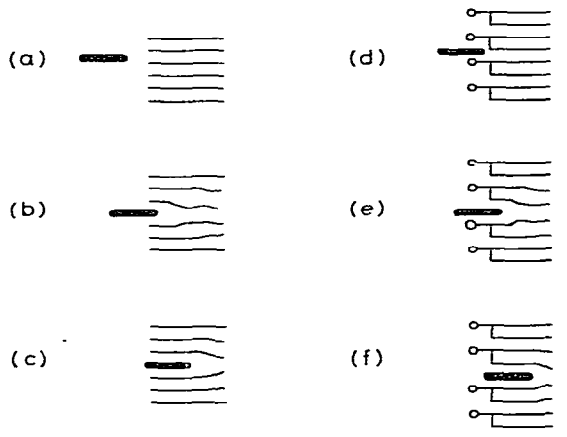

Fig. 9. Models to account for the very rapid binding of NPN to MPA. For explanation, see sect. 5.2.

NPN's water sheath is yet to come), and the perturbation and expansion of the liquid-crystalline lipid membrane. Further penetration of the guest molecule into the membrane will take it energetically "downhill", until it takes up the position of bound NPN (fig. 9c).

However, the two factors mentioned (immobilisation of NPN and expansion of the membrane) may be expected to lower the probability of attaining the transition complex, i.e., to retard the reaction. This is difficult to reconcile with our finding that the reaction is fully diffusion-controlled. It is therefore necessary to examine more closely the events at the surface.

If we take the structure of the head-group into account, then diffusion control of the binding becomes more plausible, as shown in fig. 9d. Here the incoming NPN molecule first embeds itself between the MPA head-groups, forming a loosely-held hydrophobic complex in which the area of contact between dye and membrane is quite small. Haynes and Staerk [15,16] have shown that for the system ANS/lecithin this is the only form of binding; the ANS, having a negatively-charged group, does not penetrate into the chain region but remains between the large lecithin head-groups, where its non-polar part is shielded from the water but its negative group can interact electrostatically with the lecithin dipole. The binding of ANS to lecithin is diffusion-controlled [17], and this is no surprise, since the binding consists only in diffusion of the dye into the disordered, aqueous head-group region. Ruf [18] has found a k_{on} value for the binding of *o*-methyl red

to the surface of lecithin vesicles which is also consistent with diffusion control. Thus the first step in the binding of NPN to MPA will likewise be very rapid. Once this step has been taken (fig. 9d) the NPN has lost most of its translational entropy. The next step (fig. 9e) involves penetration of the NPN into the region between the chains, which is the second endergonic and potentially rate-limiting step. However, the disruption of the lipid structure will be accompanied by reduction in the contact area between NPN and water, and the latter effect will reduce and perhaps eliminate altogether the energy barrier raised by the former. In the subsequent penetration of the dye to reach the bound position (fig. 9f) no further energy barrier is met.

Our results are supported by the unpublished observation [19] of Dr. J. Crooks that interphase diffusion in emulsions is unaffected by the presence of a fluid interfacial monolayer, but is greatly retarded by a monolayer in the crystalline state. This means that for the crystalline monolayer either k_{on} or k_{off} is greatly reduced compared with the fluid monolayer. Our demonstration (ref. [1], sect. 4.2) that K is much lower for ordered lipid membrane than for fluid suggests that the retardation of the interphase diffusion may be due to a lower k_{on} value rather than to a reduced k_{off}.

5.3. Consequences of diffusion control

If the above interpretation of the mechanism of NPN entry into MPA membranes is correct, then it will apply to the entry of any non-polar molecule and to the non-polar part of any amphiphilic molecule (fatty acids, detergents, mellitin, etc.) as long as their binding does not require a major structural rearrangement of the MPA. Similar considerations will also apply to lipids other than MPA, although it is to be expected that specific effects could arise with particular head-groups (steric hindrance, specific or preferential binding, etc.).

It is therefore to be expected that in general not only the binding of guest molecules onto the outside of a lipid membrane (as in the case of ANS and lecithin [15,16]) but also the binding of guest molecules into the membrane will be diffusion-controlled. If this also applies in the cell — and we see no reason why it should not — then it has two consequences, namely, for transport, and for the maintenance of the integrity of a membrane (which is in a sense the opposite of transport).

A plausible mechanism for the facilitation of movement within the cell of apolar molecules involves the diffusion of these molecules to a membrane and their subsequent free diffusion within the membrane [20]. Evidence for such a mechanism has been put forward [21] for the biological intermediates palmitoyl CoA and stearoyl CoA, which are synthesized by a soluble multi-enzyme complex and react subsequently with the aid of membrane-bound enzymes. The existence of this mechanism depends upon the ability of the non-polar molecules to enter the membrane rapidly, and a quantitative description of it will require a knowledge of the rate constants involved. If entry into the membrane is diffusion-controlled then it will certainly be rapid; it will also be predictable if the geometry of the system is known, since equations for the binding of substrates to membranes with subsequent diffusion and reaction have already been developed (e.g. [22]).

Although no precise reason can yet be given for the composition of any particular biological membrane, it is axiomatic that the functions of biological membranes will prove to be related to, if not determined by, their structures. If this is so then it will be important for a membrane to maintain its composition even in the presence of others of different composition. Sometimes these will be in equilibrium with each other; there is an extensive literature on phase separation in lipid membranes. At other times membranes of different structure will become mixed by the exchange of single molecules through the intervening aqueous medium. Thilo and Duckwitz-Peterlein et al. [23,24] have shown that although the equilibrium concentration of lipid monomers in solution is very small, this can be the principal mechanism for the mixing of lipid dispersions with initially heterogeneous composition. The rates they observed were consistent with diffusion-controlled escape and recombination of single molecules. The half-times for vesicle mixing are of the order of a day or more (our unpublished observations), so that long-lived cells containing membranes of differing composition which are not in equilibrium with one another must employ some means of maintaining the integrity of the various lipid phases present.

Acknowledgements

We wish to thank C.R. Rabl for expert advice in the use of the kinetic apparatus. Our thanks are further due to K. Harlos for providing electron micrographs of the vesicles, and to Dr. P. Madden, Dr. P. Tyrer and Dr. R. Schranner for valuable discussions of the theory; also to Dr. J. Crooks and Dr. L. Thilo for the communication of unpublished results and to Prof. M. Eigen for encouragement and support. P.W. acknowledges with gratitude financial support from (in chronological order) the Alexander von Humboldt Foundation, the Max Planck Society, EMBO and Magdalene College.

Appendix I

The rate of the diffusion-controlled binding reaction

A straightforward von Smoluchowski treatment for the rate of encounter and subsequent immediate reaction of two species, one of which is immobile and the other of which has a diffusion coefficient D, yields [7] eq. (A1),

$$k'_{on} = 4\pi D r L/1000 \qquad \text{(A1)}$$

where r is the radius of collision and L is Avogadro's number (the factor 1000 provides for the expression of k'_{on} in $M^{-1}\ s^{-1}$). Since the vesicle is far larger than an NPN molecule it will in comparison be practically immobile, so the eq. (A1) is appropriate to this system. For the same reason, r in the equation is to a good approximation the radius of the vesicle, assuming it to be spherical. However, it makes very little difference if the vesicle is far from spherical; it has been shown [22] that a disc-like spheroid of radius r and a cylinder-like spheroid of length $2r$ are sinks almost as efficient * as a sphere of radius r. For a very thin disc, the term 4π in eq. (A1) is replaced by the factor 8.

If the vesicle is a spherical bilayer, the number of lipid molecules in it will be given by eq. (A2), where f is the molecular area (ca. 46 $Å^2$ [1]), and r_{av} is the average radius of curvature of the vesicle (i.e., the radius of the sphere separating the outwardly- and inwardly-directed lipid molecules). θ, the fraction of the lipid molecules on the outer

$$n = (4/\theta)\pi r_{av}^2/f \qquad \text{(A2)}$$

vesicle surface, is usually close to 0.5. To a first approximation $r_{av} \approx r$, since these two radii differ only by the thickness of one monolayer of lipid, ca. 25 Å.

If on the other hand we are dealing with thin discs of bilayer structure of radius r_d, the number of lipid molecules will be given by eq. (A3).

$$n = 2\pi r_d^2/f \qquad \text{(A3)}$$

The approximate form of dependence upon particle size of the rate constant based upon the number of lipid molecules is then given by combining eqs. (A1) and (A2) and $k_{on} = k'_{on}/n$ to obtain eq. (A4) in the case of spherical vesicles ($\theta = 0.5$), while the corresponding form for discs is given in eq. (A5).

$$k_{on}(\text{spheres}) = \frac{D \cdot f}{2r} \cdot \frac{L}{1000} = 2\pi D \left(\frac{f}{2\pi n}\right)^{1/2} \frac{L}{1000} \qquad \text{(A4)}$$

$$k_{on}(\text{discs}) = \frac{4D \cdot f}{\pi r} \cdot \frac{L}{1000} = 8D \left(\frac{f}{2\pi n}\right)^{1/2} \frac{L}{1000} \qquad \text{(A5)}$$

D is given by $kT/6\pi\eta a$, where a is the radius of the guest molecule and η is the solvent viscosity [4]. Although it is possible to determine r approximately by electron microscopy, light-scattering, etc., a determination sufficiently accurate to make a good prediction of k_{on} is impossible. This uncertainty is increased by the unknown shape of the particles. Consequently the mere establishment of a particular value of k_{on} does not suffice to show that a collision reaction involving dispersed lipid is diffusion-controlled; some other criterion for this must be adopted. Eqs. (A4) and (A5) may however be used to check the consistency of the experimental data (see Discussion), although the check is not a sensitive one.

It is germane at this point to draw attention to a significant difference between diffusion-controlled and non-diffusion-controlled kinetics in these systems. If the binding reaction is represented as eq. (A6), where MPA is in considerable excess over NPN, then eq. (A7) follows (C_L = concentration of lipid).

* From ref. [22], if electrostatic effects on the rate of the diffusion-controlled reaction are absent, then the relative efficiencies are: sphere, 100%; extremely flat disc, 64%; cylinder, 33% for a length: diameter ratio of 10:1.

$$NPN_{free} + MPA \rightleftharpoons NPN_{bound} \quad (A6)$$

$$K = \frac{[NPN_{bound}]}{[NPN_{free}]} \times \frac{1}{C_L} = \frac{K'}{n} \quad (A7)$$

Now, since both for spherical and for disc-shaped particles n is directly proportional to the square of the radius, it follows that K' is proportional to the radius squared if K is independent of the particle's radius. This is in accordance with the usual qualitative pictures of the binding of an organic molecule to an excess of a lipid membrane: the volume of the oil phase into which the guest molecule can partition (*or* the number of binding sites on the membrane) is proportional to the area of a membrane of given constitution (*or* to the number of molecules providing binding sites), so that K, based on the number of lipid molecules, is independent of the particle size, whereas K', based upon the number of vesicles, is proportional to the area (*or* number of molecules) of the vesicle.

In consequence of this the radius dependences of the apparent rate constants for diffusion-controlled and non-diffusion-controlled conditions will differ from one another. If the "on" step is not diffusion-controlled, then k'_{on} will be proportional to the target area of the lipid vesicle, i.e., to r^2 (see eq. (5a); K'_1 is proportional to r^2), whence k'_{off} is independent of r. Under diffusion control, however, k'_{on} is proportional to the radius r (eq. (A1)), so that invoking the relationship $K' = k'_{on}/k'_{off}$, we see that k'_{off} is inversely proportional to r. For spherical vesicles undergoing diffusion-controlled reaction the expression for the reverse rate constant k'_{off} is given by eqs. (A8) and (A9).

$$K' = \frac{k'_{on}}{k'_{off}} = \frac{4\pi r^2 K}{\theta f} \quad (A8)$$

$$k'_{off} = k_{off} = \frac{\theta D f}{rK} \cdot \frac{L}{1000} \quad (A9)$$

The reason for the dependence of k'_{off} upon $1/r$ is not immediately clear, but the following considerations provide some insight: k'_{off} equals k'_{-1}/K'_2 (eqs. (2a) and (4a)), and $K' = K'_1 K'_2$. It is easily shown that the stability constant K'_1 for formation of the encounter complex is proportional to r^2 in the absence of electrostatic interactions and if r is large compared to the size of a dye molecule. Since K' is proportional to r^2, it follows that K'_2 is independent of r (at least for the concentrations conditions considered here) and that the $1/r$-dependence of k'_{off} is due to k'_{-1}.

This is confirmed by the following calculation. If $n(x, t)$ is the concentration of dye molecules at a distance x from the centre of the vesicle (assumed spherical, radius r) at time t, then the diffusion equation for the system in polar coordinates is given by eq. (A10).

$$\frac{\partial(xn)}{\partial t} = D \frac{\partial^2(xn)}{\partial x^2} \quad (A10)$$

D is the diffusion coefficient of the dye. This is solved in the von Smoluchowski treatment for the association reaction with a uniform concentration n_0 at time ($t = 0$); this becomes depleted by reaction and a concentration gradient is set up which reaches a steady state ($n(r, t) = 0$; $n(\infty, t) = n_0$ (e.g. [7])). To evaluate k'_{off} we adopt different boundary conditions: initially the concentration of dye is zero except at the very surface of the membrane, at a distance r from the centre of the vesicle; this concentration is denoted by n_0 and considered to be constant. Solving eq. (A10) with the boundary conditions $n(r, t) = n(r, 0) = n_0$, $n(x, 0) = 0$ for $x > r$ and $n(\infty, t) = 0$ yields (cf. refs. [7,25]) eq. (A11) as an exact solution, which leads to $(\partial n/\partial x)_{x=r} = -(n_0/r) - n_0/\sqrt{\pi D t}$.

$$n(x, t) = n_0 \left[\frac{r}{x} - \frac{2r}{x\sqrt{\pi}} \int_0^{(x-r)/2\sqrt{Dt}} \exp(-w^2)\, dw \right] \quad (A11)$$

The rate of departure from the surface of one vesicle is therefore by Fick's law given by eq. (A12), in which N denotes number of moles and n_0 is expressed in mole/cm^3.

$$dN/dt = 4\pi r^2 \cdot D[n_0/r + n_0/\sqrt{\pi D t}] \quad (A12)$$

The second term on the right is negligible when t is greater than 1 μs (for $r = 100$ Å and $D = 10^{-5}$ cm^2 s^{-1}). Extending to 1 litre of our solution we obtain eq. (A13).

$$d[NPN_{free}]/dt = 4\pi r \cdot D \cdot n_0 \cdot L[Ves] \quad (A13)$$

Here the question arises as to the actual value of n_0. Two assumptions might be considered:

i) It is assumed that at the surface of the vesicle a thin layer of solution exists in which the concentration of dye is that of an aqueous medium at equilibrium with the bound dye, the concentration being maintained *via* the rapid pre-equilibrium K'_2. This means,

n_0 in eq. (A13) is substituted by $[NPN_{free}]/1000$. With eq. (A7) the relationship $C_L = n[Ves]$ and eq. (A2), rearrangement leads to eq. (A14).

$$\frac{d[NPN_{free}]}{dt} = \frac{\theta f D L}{r K 1000} [NPN_{bound}] \qquad (A14)$$

Thus $k'_{off} = \theta f D L / r K 1000$, which is identical to the expression derived above (eq. (A9)) by consideration of the equilibrium.

ii) In models of diffusion-controlled separation processes the concentration of the particles diffusing away from the reaction centre is usually assumed to be (and to be maintained) 1 molecule per centre [26]. Normally this corresponds to $1/\frac{4}{3}r^3\pi$ molecules per cm^3 or $n_0 = 3/4r^3\pi L$ mole/cm^3. In our case, however, with a very large vesicle as centre, a molecule is considered to be associated when it is within a certain distance d ($\ll r$) of the vesicle's surface, i.e. within a layer of volume $4r^2\pi d$. In our case the concentration at $x = r$ may therefore be taken as $1/4r^2\pi \cdot d$ molecules per cm^3 or $n_0 = 1/4r^2\pi d L$ mole/cm^3. With the concentration conditions of this study it is indeed most unlikely that more than one NPN molecule is within that layer. Substituting this value of n_0 into eq. (A13) yields eq. (A15).

$$d[NPN_{free}]/dt = (D/r d)[Ves] \qquad (A15)$$

In this expression [Ves] actually stands for the concentration of NPN-Ves associations, i.e. for [EC] (sect. 5.1.1). Thus the rate constant for the diffusion-controlled separation of these aggregates is given by $k'_{-1} = D/r d$, showing the $1/r$-dependence mentioned above. For instance, if we assume $D = 10^{-5}$ cm^2 s^{-1}, $r = 200$ Å and $d = 8$ Å, then $k'_{-1} = 6 \times 10^7$ s^{-1}. This expression for k'_{-1} is also obtained, more directly, by combining the expression for $k'_1 = k'_{on}$ given by eq. (A1) with the expression for the stability constant $K'_1 = k'_1/k'_{-1}$ of the encounter complex EC, for which a simple statistical consideration (no electrostatic interactions involved) gives eq. (A16) ($[NPN_{assoc}] = [EC]$).

$$K'_1 = \frac{[NPN_{assoc}]}{[NPN_{free}][Ves]} = \frac{4r^2\pi d \cdot L}{1000} \qquad (A16)$$

Appendix II

Relaxation time of dye binding in the presence of a distribution of vesicle sizes

For the simple binding reaction shown by eq. (1) in which conditions are such that the concentration of bound NPN is always much less than that of MPA, the expression for the relaxation time may easily be derived, eq. (2a).

It was shown above (sect. 5.1.2) that the "on" step is a diffusion-controlled process and that in such a situation both rate constants k'_{on} and k'_{off} are functions of the radius of the vesicles (appendix I). Therefore, when a size distribution of vesicles is present (as is to be expected), the relaxation behaviour is actually more complex than indicated by eq. (2a). The following considerations apply to this situation.

The vesicles are considered to be "sorted" according to their size r_i into N groups, and the reaction of each group with the dye is considered as a separate reaction, eq. (A17).

$$I + V_i \underset{k_{-i}}{\overset{k_i}{\rightleftharpoons}} I_i^* \qquad (i = 1 \ldots N) \qquad (A17)$$

In this (short-hand) notation I represents free, aqueous indicator dye (= NPN_{free}), V_i represents a vesicle of size r_i, I_i^* represents the dye bound to a vesicle of size r_i (= $NPN_{bound(i)}$), and k_i (= $k'_{on(i)}$) and k_{-i} (= $k'_{off(i)}$) are the rate constants appropriate to vesicles of size r_i. This set of coupled reactions is described by the rate equations (A18).

$$d[I_i^*]/dt = k_i[V_i][I] - k_{-i}[I_i^*] \qquad (i = 1 \ldots N) \qquad (A18)$$

The relaxation process is then characterized by a system of differential equations for which — with the mass balance equation $\Delta[I] + \Sigma_{i=1}^{N} \Delta[I_i^*] = 0$ and with $[V_i] = \text{const}$ (sect. 5.1.1) — expression (A19) is obtained.

$$\frac{d(\Delta[I_i^*])}{dt} = -k_i[V_i] \sum_{j=1}^{N} \Delta[I_j^*] - k_{-i}\Delta[I_i^*] \qquad (i = 1 \ldots N) \qquad (A19)$$

The eigenvalues of this system of differential equations are given by the solutions of the determinant (A20),

$$|a_{ij} - \lambda\delta_{ij}| = 0 \qquad \text{(A20)}$$

where δ_{ij} is the Kronecker delta (i.e. $\delta_{ij} = 1$ for $i = j$ and $\delta_{ij} = 0$ for $i \neq j$), and the terms a_{ij} are given by $a_{ij} = -k_i[V_i] - k_{-i}\delta_{ij}$. Since the negative reciprocal eigenvalues represent the relaxation times of the system, we may write equation (A21).

$$|k_i[V_i] + (k_{-i} - \tau^{-1})\delta_{ij}| = 0 \qquad \text{(A21)}$$

It follows that the relaxation process is characterized by a spectrum of N relaxation times for which, however, there is no general solution.

Simple solutions are obtained only in the special cases in which $[V_i]$ is either very high or very low, so that of the sums $(k_{-i} + k_i[V_i])$ either k_{-i} or $k_i[V_i]$ may be neglected, leading to eqs. (A22) and (A23).

$$|k_i[V_i] - \tau^{-1}\delta_{ij}| = 0 \qquad \text{(A22)}$$

$$|k_i[V_i](1 - \delta_{ij}) + (k_{-i} - \tau^{-1})\delta_{ij}| = 0 \qquad \text{(A23)}$$

Eq. (A22) has $(N - 1)$ roots whose value is zero and one root with a value given by eq. (A24).

$$\tau^{-1} = \sum_{i=1}^{N} k_i[V_i] \qquad \text{(A24)}$$

(This becomes immediately apparent by inspection of eq. (A19): if the $k_{-i}\Delta[I_i^*]$ are neglected, each differential equation differs from any other only by a numerical factor. Summing all equations leads directly to (A24).) Thus a distribution of vesicle sizes will in this extreme case show a single exponential relaxation curve, i.e. one which corresponds to a single time constant. The condition for this, $k_i[V_i] \gg k_{-i}$, simply means that the binding equilibrium (eq. (1)) is predominantly over to the right-hand side, a condition realised when $C_L \gg 1/K$, i.e. at most lipid concentrations used in the kinetic experiments. The lowest value of C_L employed was 5×10^{-5} M, approximately equal to $1/K$.

At very low lipid concentrations, eq. (A23) applies. Each different size of vesicle, with its corresponding k_{-i} value, will produce a separate root of value $\tau_i^{-1} = k_{-i}$. Therefore, the relaxation process at very low lipid concentrations is characterized by the superposition of N exponential functions with different time constants. Consequently the relaxation function at low lipid concentrations will not be exponential, even for very small perturbations of the equilibrium.

References

[1] P. Woolley, Biophys. Chem. 10 (1979) 289.
[2] R. Rigler, C.R. Rabl and T.M. Jovin, Rev. Sci. Instrum. 45 (1974) 580.
[3] H. Träuble, M. Teubner, P. Woolley and H. Eibl, Biophysical Chem. 4 (1976) 319.
[4] D.N. Hague, Fast reactions (Wiley-Interscience, 1971) pp. 12–14 and 144–146.
[5] M. Eigen and L. de Maeyer, in: Technique of organic chemistry, ed. A. Weissberger, Vol. VIII, Part II (2nd Edn., Interscience, 1963) pp. 895–1054.
[6] W.P. Jencks, Catalysis in chemistry and enzymology (McGraw-Hill, 1969) pp. 605–607.
[7] E.A. Moelwyn-Hughes, Physical chemistry (2nd Ed., Pergamon, Oxford, 1961) pp. 1207–1212.
[8] E.F. Caldin and B.B. Hasinoff, J.C.S. Faraday I (1975) 515.
[9] R.M. Noyes, Prog. Reaction Kinetics (Pergamon, London) 1 (1961) 129.
[10] E.F. Caldin, Fast reactions in solution (Blackwell, Oxford, 1964) p. 11.
[11] C.R.C. Handbook of Chemistry and Physics, ed. R.C. Weast (57th Ed., C.R.C. Press, 1976) p. F-51.
[12] G.W. Castellan, Ber. Bunsenges. Physik. Chem. 67 (1963) 898.
[13] D. Thusius, Biophysical Chem. 7 (1977) 87.
[14] M. Eigen, Angew. Chem. 75 (1963) 489.
[15] D.H. Haynes and H. Staerk, J. Membrane Biol. 17 (1974) 313.
[16] D.H. Haynes, J. Membrane Biol. 17 (1974) 341.
[17] D.H. Haynes and P. Simkowitz, J. Membrane Biol. 33 (1977) 63.
[18] H. Ruf, Mechanism of carrier-mediated proton transport across lipid bilayer membranes, (to appear in J. Membrane Biol.).
[19] J. Crooks (King's College, London) to be published.
[20] G. Adam and M. Delbrück, in: Structural chemistry and molecular biology, eds. N. Davidson and A. Rich (W.H. Freeman, San Francisco (1968) p. 198.
[21] M. Sumper and H. Träuble, F.E.B.S. Lett. 30 (1973) 29.
[22] P.H. Richter and M. Eigen, Biophysical Chem. 2 (1974) 255.
[23] G. Duckwitz-Peterlein, G. Eilenberger and P. Overath, Biochim. Biophys. Acta 469 (1977) 311.
[24] L. Thilo, Biochim. Biophys. Acta 469 (1977) 326.
[25] I. Sneddon, Elements of partial differential equations (McGraw-Hill/Kogakusha, 1957) pp. 282–285.
[26] M. Eigen, Z. Physik. Chem. N.F. 1 (1954) 176.